

RESEARCH ARTICLE

Joint spatial modelling of malaria incidence and vector's abundance shows heterogeneity in malaria-vector geographical relationships

Ruth Marie A. Kouame^{1,2} | Ako V. Constant Edi¹ | Russell John Cain³ |
David Weetman⁴ | Martin James Donnelly⁴  | Luigi Sedda³ 

¹Centre Suisse de Recherches Scientifiques en Côte d'Ivoire, Abidjan, Côte d'Ivoire

²Institut National Polytechnique Félix Houphouët Boigny, Yamoussoukro, Côte d'Ivoire

³Lancaster Ecology and Epidemiology Group, Lancaster Medical School, Lancaster University, Lancaster, UK

⁴Department of Vector Biology, Liverpool School of Tropical Medicine, Liverpool, UK

Correspondence

Luigi Sedda
Email: l.sedda@lancaster.ac.uk

Funding information

Medical Research Council, Grant/Award Number: MR/P02520X/1; EDCTP2 Programme; Wellcome Trust NIHR-Wellcome Partnership for Global Health Research Collaborative Award, Grant/Award Number: 220870/Z/20/Z; Royal Society Wolfson Fellowship, Grant/Award Number: RSWF\FT\180003

Handling Editor: Martin Nuñez

Abstract

1. Limited attention from the modelling community has been given to ecological approaches which aim to predict geographical patterns of malaria by accounting for the joint effects of different vectors and environmental drivers.
2. A hierarchical multivariate joint spatial Gaussian generalised linear model was developed to provide joint parameters inference and mapping of counts of *Anopheles gambiae*, *An. funestus*, *An. nili* and malaria incidence collected in an area of Cote d'Ivoire. Variable-selection methods were applied to select important predictors for each mosquito species and malaria incidence.
3. The proposed joint model led to a general reduction of the variance in the estimates compared to independent modelling. There was high variability in the composition of *Anopheles* mosquito species in the villages with each species suitability only partly overlapping geographically.
4. Abundances of *An. gambiae*, *An. funestus* and *An. nili* were primarily determined by temperature. None of the species were found as a significant predictor for the others. *Anopheles gambiae* was the predominant species and only *An. gambiae* female abundance was an important variable (linear predictor) for malaria incidence. However, the geographic correlation analyses show that the rest of *Anopheles* species are likely playing a role in malaria suitability.
5. Residuals from the models of mosquito abundance and malaria cases are also correlated with each other and overlapping but in geographic patches, meaning that local drivers of vector-malaria suitability are still present and not represented by the predictors used in the model.
6. *Synthesis and applications:* Joint modelling improve predictive estimation compared to individual modelling. The accurate predictions highlighted high diversity in the association between malaria and vector species, with most of the area having more than one species suitability correlated with malaria suitability. These zones are unlikely to benefit from species-specific interventions. Areas with

This is an open access article under the terms of the [Creative Commons Attribution](https://creativecommons.org/licenses/by/4.0/) License, which permits use, distribution and reproduction in any medium, provided the original work is properly cited.

© 2023 The Authors. *Journal of Applied Ecology* published by John Wiley & Sons Ltd on behalf of British Ecological Society.

correlated malaria and vector species suitability residuals contain local information, not included in the model, that requires further investigation. This will identify additional communal malaria and vectors factors that need to be considered for optimal malaria control and elimination strategies since these factors are expected to be linked to the local malaria transmission.

KEYWORDS

Anopheles, co-occurrence mapping, geostatistics, joint vector-disease modelling, malaria, remote sensing, targeted interventions

1 | INTRODUCTION

Despite a major decrease in malaria cases in the last two decades, the progress has stalled since 2015 (Noor & Alonso, 2022) and malaria remains the most important vector-borne disease in Africa (World Health Organization, 2022). Malaria has a significant socio-economic impact in Côte d'Ivoire (Tchicaya et al., 2014); in fact, despite more than 50% of the population having access to long-lasting insecticide-treated nets (LLINs) or indoor residual spraying (IRS; World Health Organization, 2020), approximately 8 million cases of malaria were reported in 2018 (the same year of this field study; World Health Organization, 2019). In Côte d'Ivoire, and West Africa generally the main malaria vectors are *Anopheles arabiensis*, *An. coluzzii*, *An. funestus* and *An. gambiae* though their relative importance varies in space and time (Adja et al., 2011).

Environmental factors are major drivers of mosquito and malaria distribution (Dossou-yovo et al., 1995). For this reason, differences and similarities in environmental effects for each vector and malaria can be implemented in joint models in which individual models for malaria and vectors are optimised together by defining statistical dependencies between the individual models rather than being optimised independently. One of these dependencies is the explicit spatial correlation, that is malaria and vectors have their own spatial variation, part of which may be considered shared between them. Understanding this shared variation is the focus of this study with the aim to improve targeted surveillance and control by delineating areas that can be prioritised for interventions based on the number of vectors involved and their relative risk, and areas in need of future sampling and investigation in terms of local factors (Finley et al., 2014; Liu et al., 2017) that were missed in the modelling but that contributes at the local malaria transmission. The identification of this shared component is mostly neglected in previous literature, but is key for detailed understanding of the spatial patterns in the interactions between malaria and vectors. For this reason, we have developed a framework for joint Gaussian spatial processes (FJGS) as a hierarchical multivariate joint spatially-explicit Gaussian generalised linear model to capture and quantify shared spatial and individual risk factors effects (for mosquitoes species and malaria). This was followed by the co-regionalisation analyses of vectors and malaria suitabilities, to identify geographical clustering of common drivers and hidden local risk factors that can inform geographically targeted

interventions (Attoumane et al., 2020; Handique et al., 2016; Russell et al., 2013; Zhou et al., 2007). Co-regionalisation between vectors and malaria predicted by both fixed effects (the proportion of variance explained by the environmental variables) and residuals has not been investigated before for malaria.

This analysis is applied to field data collected from the region of Agboville in Côte d'Ivoire, an endemic malaria area with different *Anopheles* vectors playing a role in the local malaria transmission although poorly understood.

2 | MATERIALS AND METHODS

2.1 | Study area

Agnéby-Tiassa region, southern Côte d'Ivoire, is divided into four departments: Agboville, Taabo, Tiassalé and Sikensi (Figure 1). This region is located in the evergreen forest zone with altitude between 30 and 100m above sea level. The climate is characterised by four seasons: a long rainy season (April–July), a short dry season (August–September), a short rainy season (October–November) and a long dry season (December–March). Average temperature is around 27°C and average rainfall is 120mm. Relative humidity ranges from 70% to 85%. The region is characterised by a diverse hydrographic network dominated by the Bandama and N'zi rivers. The primary activity of the rural population is agriculture, focused on cocoa, rubber, vegetable and irrigated rice fields, usually with heavy use of pesticides. Malaria transmission occurs mainly during the rainy seasons, between April and November.

2.2 | Entomological collections

Entomological collections were carried out from September to November 2018 following an optimised ecological spatial sampling design described in Sedda et al. (2019). Within this framework, 30 villages were selected within an area of 60 by 60km (Figure 1). A total of 120 houses (four houses per village) were randomly selected for mosquito collection.

Mosquitoes were collected during four consecutive nights every 2 weeks for 10 weeks (five collection rounds in total), using CDC light

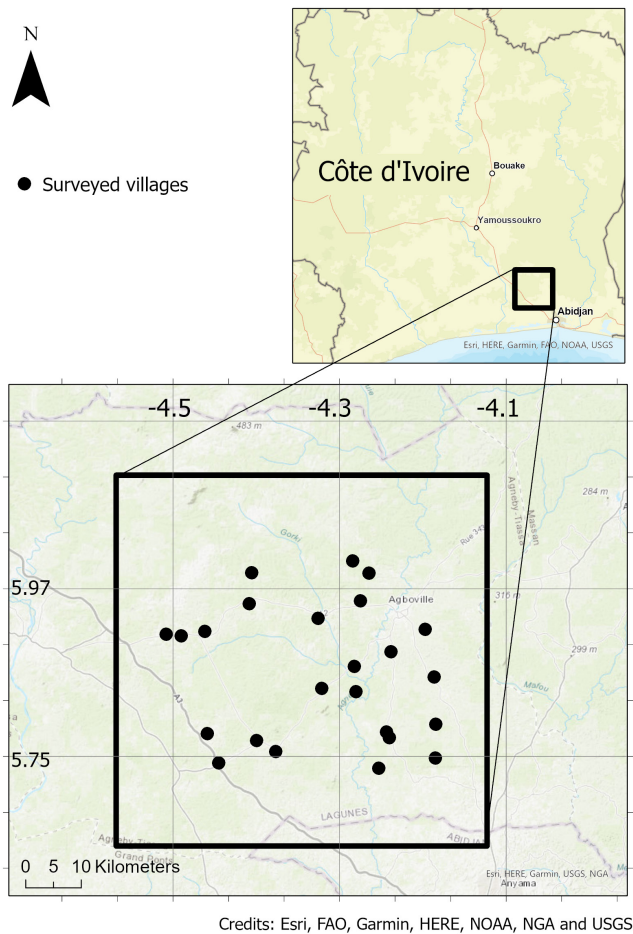


FIGURE 1 Study area and survey locations. Each of the 30 survey locations include four houses which are sampled for mosquito collection. Background from OpenStreetMap under the Open Database licence (<https://www.openstreetmap.org/copyrigh>).

traps (Model 512, John W. Hock Company, Gainesville, FL) making a total number of 600 collection records (4 houses \times 30 villages \times 5 collection times; Kouame & Edi, 2023).

For each village, a member of the community was trained in the use of the traps and sampling protocol. The order of house collection was randomised before each collection to remove systematic biases. Traps were positioned at a height of 1.5 m in sleeping rooms and operated on 12-V battery power from 8:00 PM to 6:00 AM. Each morning, mosquitoes were collected, stored in ziplock bags containing silica gel and transported immediately to the laboratory of the Centre Suisse de Recherches Scientifiques in Tiassalé for morphological identification using available keys in the literature (Becker et al., 2010; Gillies & Coetzee, 1987).

2.3 | Malaria incidence collection

Malaria incidence, confirmed malaria cases and census population size of each sampled village were obtained from the regional public health centre of the department of Agboville. Malaria information

for 2018 was available for 17 rural public health centres covering 25 out of 30 villages.

2.4 | Environmental variables

Environmental data were sourced from both satellite and weather stations at different spatial resolutions in order to account for different scale effects (see Table S1 in Supporting Information). For each village in the study, hourly climatic data were used to calculate weekly averages, minima and maxima at 500-m resolution (see Table S1). We also included 30-m resolution global land cover classification (an alternative at higher spatial resolution is available at <https://2016africallandcover20m.esrin.esa.int/>), satellite-detected elevation and bioclim precipitation. Moderate resolution imaging spectroradiometer (MODIS) satellite products monthly temperature, enhanced vegetation index (EVI) and the ratio of actual to potential evapotranspiration (ET) were included in the dataset. Finally, for all the variables with the exception of land cover, bioclim precipitation and elevation, amplitude and variance at their original spatial and temporal scales were calculated. Amplitude is a measure of the overall variability, therefore large values are associated with large fluctuations. All these variables may have a direct or indirect link with the presence of malaria vectors (Lindsay & Bayoh, 2004) and with malaria incidence in West Africa (Arab et al., 2014). Entomological and environmental predictors were employed in the variable selection step, and those found important were included in the main model.

2.5 | Ethical approval and field study permissions

The malaria database provides aggregated counts only and not individual data, and this did not require ethical approval. For the entomological collections, households were informed about the purpose of the survey and a consent form was read and signed by the heads of each household before the entomological collection was conducted in their houses. The ethical approval for entomological collection was obtained from the Comité National d'Ethique des Sciences de la Vie et de la Santé (reference number 168-18/MSHP/CNESVS- km). Ethical approval for secondary data analyses was obtained from the Faculty of Health and Medicine Research Ethics Committee at Lancaster University (UK) with reference number FHMREC20173. This research did not involve animals or interviews with human participants and therefore relevant ethical approvals were not necessary. Field work did not need appropriate licences and/or permits, apart from the approved ethical application for the entomological collection described above.

2.6 | Statistical analysis

The statistical model herein considers each of the three different *Anopheles* spp. (*An. gambiae*, *An. funestus* and *An. nili*) collected in this

study as a separate Gaussian generalised linear model, as well as malaria incidence for a total of four models. These models are parameterised jointly assuming a common unknown spatial process, that is, all the models employ the same spatial autocorrelation function.

Predictors are identified by important variable selection (described below) for each of the four models separately. Once important variables were found, the analysis carried on with joint modelling of the vectors and malaria models, followed by model evaluation, validation and analysis of co-regionalised vector and malaria distributions and co-regionalised residuals. Two vectors or a vector and malaria are co-regionalised if their suitability (or residuals) overlap in a region. Overlapping is expressed as positive correlation in the suitability values.

Statistical analysis was performed in R-cran software (V.4.0.4) with packages MuMIn for model selection, bmstdr and spbayes for model inference and prediction and coda for convergence testing. Each statistical analysis is described in more detail below.

2.6.1 | Variable selection

Collinearity is common among ecological variables and can lead to poor model selection through variable redundancy. Prior to variable selection, we removed those variables with Pearson's correlation coefficient with other predictors above an absolute value of 0.6 which is a conservative value compared to the value of 0.7 usually applied in ecology and found to be a good approach for collinearity in ecological studies (Dormann et al., 2013). Of the 60 predictors, six were found collinear with other variables and then removed, keeping those with higher significance in the predictor's coefficient and explained variance, and lowest AIC in univariate general linear models. For each model, we conducted a variable selection analysis by testing all the possible combinations of the remaining 54 predictors (36 environmental variables, 2 *Anopheles* and 16 other mosquito species and sex) within a spatial Gaussian generalised linear model (statistical form described in the next section). The model with the lowest Watanabe-Akaike information criterion value (WAIC) is considered to be the best fitting (Gelman et al., 2014). WAIC is designed for Bayesian analyses and averages over the posterior distribution rather than conditioning on a point estimate as in other measures (Ploton et al., 2020). The variable selection method used in this work is based on a model type that is also employed in the joint modelling to maintain consistent results between the variable selection step and the joint modelling. Alternative methods include the use of machine learning with spatial cross validation to account for spatial autocorrelation in the outcome (Meyer et al., 2019).

2.6.2 | Joint modelling

The FJGS was implemented within a Bayesian hierarchical multivariate joint spatially-explicit Gaussian generalised linear model

(Sedda, 2023). FJGS was used to model each of the three *Anopheles* species' log counts and malaria incidence as four spatially dependent processes (in other words, mosquito species and malaria are dependent on the distance between sampling locations) with common spatial structure. Using vectorised notation for a spatial model with nugget effects (as in section 6.5 of Sahu, 2022), the multivariate model can be expressed as

$$\log(y_j) | \omega \sim N(\mathbf{X}_j \beta_j + \omega, \epsilon)$$

$$\omega \sim N(0, \sigma^2 \mathbf{H})$$

$$\epsilon \sim N(0, \tau^2 \mathbf{I})$$

where \mathbf{X} is the design matrix containing the values of the covariates, β are unknown regression coefficients, ω is a zero mean Gaussian process with exponential covariance function (\mathbf{H}) with unknown parameters common to all models, σ^2 is the spatially dependent variance, ϵ is the pure error term or nugget effect, common to all models, which follow an independent zero mean normal distribution with variance τ^2 , and \mathbf{I} is the identity matrix. The correlation matrix \mathbf{H} has elements obtained from the exponential function:

$$h = \exp(-\delta / \varphi)$$

where δ is the distance separating two locations and φ the spatial range also known as spatial decay parameter (the distance at which the variance or autocorrelation between two locations is no longer dependent on the distance between the two locations (Cressie, 2015), or in other words, the distance at which the spatially dependent variance is equal to the sample variance).

The full Bayesian model specification has vague priors for all parameters, including the spatial term:

$$\beta_j \sim N(\beta_{0j}, \mathbf{M}^{-1})$$

$$\lambda_\sigma^2 = \frac{1}{\sigma^2} \text{ and } \lambda_\tau^2 = \frac{1}{\tau^2}$$

$$\lambda_\sigma^2 \sim \text{Gamma}(a, b)$$

$$\lambda_\omega^2 \sim \text{Gamma}(p, q)$$

$$\varphi \sim U(u, v)$$

where β follows a multivariate normal distribution with mean β_0 and precision matrix \mathbf{M}^{-1} , the precisions for the variances τ^2 and σ^2 , λ_σ^2 and λ_ω^2 respectively, are Gamma distributed with shape parameters a and p and scale parameters b and q . The spatial decay parameter φ is uniformly distributed with minimum u and maximum v distance limits.

Finally, the regression model applied on this study can be also written as

$$\log(y_{j,s}) = \text{Time} + x_{j,s}^T \beta_j + \omega_s + \epsilon_s, j = 1, \dots, J$$

with subscripts j :

$j=1$ for *Anopheles gambiae*; $j=2$ for *Anopheles funestus*; $j=3$ for *Anopheles nili*; $j=4$ for malaria incidence in humans.

s is the spatial location (i.e. longitude and latitude). *Time* is an offset term expressed in week of survey ($\text{Time}=1, \dots, 5$).

Posterior distributions were generated from an adaptive Markov Chain Monte Carlo (AMCMC) algorithm (Finley et al., 2015) that updates tuning parameters as it runs. The AMCMC algorithm preserves ergodicity and returns valid and effective results (Rosenthal, 2007). The AMCMC runs within a Metropolis-Hastings framework (Sahu, 2022). Joint modelling is obtained through the ω specification, forced to be common to all four models and optimised using a metabayes approach (AlShammari et al., 2021; Figure 2), where the priors of the ω and ε distributions and β_0 parameters are updated every t MCMC chain block (fixed to $t=1000$). Acceptance is constrained to maximisation of the likelihood in at least three out of four models, in order to avoid being stuck in a local optimum. The AMCMC were run for 100,000 iterations after a burn-in of 20,000 iterations. Convergence was assessed via Gelman and Rubin's potential scale reduction factor convergence diagnostics, as well as the Geweke time series statistic (Plummer et al., 2006). We calculated 95% credible intervals for each parameter estimate (equal-tailed intervals).

The prior specifications, some of them based on cross-validation and acceptance rate tests, are: \mathbf{M}^{-1} is a diagonal matrix with diagonal values equal to 0.1, β_0 are initially fixed as

coefficients obtained from a non-spatial generalised linear model and later updated during the inference, $a=2$ and $b=1$ allow for finite mean and not-finite variance to have a vague gamma distribution (Sahu, 2022), similarly for $p=2$ and $q=0.1$. a , b , p and q are updated during the inference. u and v are initially selected as the 2.5% (u) and 97.5% (v) quantile of the distances among all locations. u and v are updated during the inference.

2.6.3 | Model evaluation

Model evaluation was performed with the analysis of observed versus predicted values for each model via mean error and mean squared error. In addition, robustness of the model was assessed using cross-validation by leaving out 15% of the data (Vehtari et al., 2017) with similar spatial dependence (Roberts et al., 2017). In addition, we performed a leave-one-village-out cross validation repeated for all villages (Meyer et al., 2018). In other words, at each cross validation, the data from one village were left-out, the model was trained with the other 29 villages and the predictive performance of the model was assessed on the left-out village. Cross validation assessment was carried out by measuring the root mean square error and coverage. Coverage does not measure discrepancy but estimates the proportion of cross-validation left-out values that follow within the predicted MCMC samples. As suggested by Sahu (Sahu, 2022), an ideal value of coverage is 95%;

$$\theta = (\beta_0, a, b, p, q, u, v)$$

$\dot{\theta}$ = initial status or unchanged status

$\hat{\theta}$ = transient status

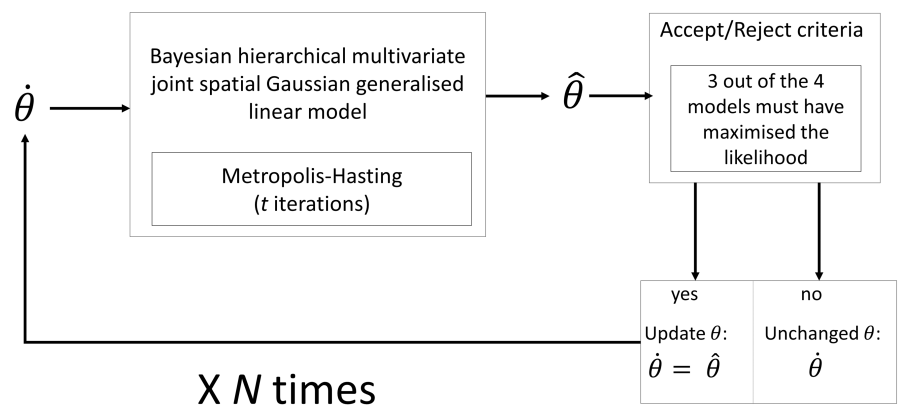


FIGURE 2 Metabayes approach used to optimise joint parameters.

$$N = \frac{\text{total number of iterations} - \text{burn in}}{t \text{ chain blocks}}$$

higher values may be due to an excessively wide MCMC prediction sample interval. In addition, we used the same validation statistics to compare the joint model with the independent models, to evaluate if a joint approach is better than running four independent models.

2.6.4 | Co-regionalisation analysis

Local correlation between estimated suitability of each vector and malaria, and between their residuals, was obtained from moving window correlation analyses. Around each grid node, a 5 by 5 km window (yielding a total of 10 by 10 cells within the grid resolution of 500m) was superimposed to extract the estimated values of suitability or residuals for the vector and malaria. Once the two datasets (suitability or residuals values for vector and suitability or residuals values for malaria) were created, the Pearson's correlation was calculated and mapped.

In addition, we delineate areas of high risk as those with suitability greater than 0.25 for both the vector and malaria and a correlation larger than 0.1.

3 | RESULTS

3.1 | Summary statistics

The mosquito genera trapped during the surveillance were *Anopheles* (45.51%), *Culex* (29.04%), *Mansonia* (22.68%) and *Aedes* (2.76%). Species identified were *An. gambiae*, *An. nili*, *An. funestus*, *C. nebulosus*, *C. quinquefasciatus*, *C. weschei*, *M. uniformis*, *M. Africana*, *A. palpalis*, *A. vitatus* and *A. aegypti*. All identified mosquitoes are included in the analysis as predictors, and only *Anopheles* are considered as response variables. For *Anopheles*, only female counts are used owing to very few males being trapped (Table 1). *Anopheles gambiae* was present in 90% of the villages, *An. nili* in 27% and *An. funestus* in 17% of the villages (see Table S2).

Anopheles gambiae was caught in 69% of houses, with *An. funestus* and *An. nili* being trapped in 8.5% and 12% of houses, respectively. The three species were never collected together at the same

time in the same house; 52% of the house collections yielded one *Anopheles* species, 18% two species and 30% did not collect any species. A high degree of spatial heterogeneity for mosquito species and their counts was found across the area and even at short distances (Figure 3b–d), while malaria incidence is homogeneously distributed but not in the centre-west of the region (Figure 3a). *Anopheles gambiae* had the largest collection which increased over time (see Figure S1).

3.2 | Important environmental predictors

Out of the 54 predictors used in the variable selection, four were selected for *An. gambiae*, two for *An. funestus*, one for *An. nili* and three for malaria incidence (Table 2). Temperature is the predictor (risk factor) common to both vectors and malaria (although different in nature since some of the temperature predictors are satellite-based, and others are from weather stations; Table 2). Apart from temperature, the four models show different important variables which reflect their different spatial patterns. Other risk factors for *An. gambiae* included land cover, with grassland (lands covered by natural grass with cover density over 10%) increasing the number of mosquitoes trapped when compared to forest (lands covered with trees, the top density of which covers over 10%), while wind speed and elevation decreased *An. gambiae* catches. Female *Mansonia uniformis* mosquito counts were a predictor for female *An. funestus*; while the number of female *An. gambiae* and vegetation biomass amplitude (i.e. variability in vegetation, which may be a proxy for land cover changes) for malaria incidence. Therefore, for malaria incidence, the only mosquito species predictor selected by the model is *An. gambiae* female counts (Table 2). In general, none of the variables are shared between mosquito species. Malaria incidence and *An. gambiae* female share the same temperature variable.

Three predictors show wide credible intervals while keeping their statistical significance: land cover, wind speed and *An. gambiae* female counts. This means a higher uncertainty in the contribution of these variables to their relative outcome (land cover and wind speed for *An. gambiae*, and *An. gambiae* female counts for malaria incidence) since their credible intervals contain values that can double or halve the outcome.

	Min.	Median	Mean	Max	Sum (total trapping)
<i>An. gambiae</i> ♀	0	0	6.472	418	3883
<i>An. gambiae</i> ♂	0	0	0.010	1	6
<i>An. funestus</i> ♀	0	0	0.028	3	17
<i>An. funestus</i> ♂	0	0	0	0	0
<i>An. nili</i> ♀	0	0	0.085	9	51
<i>An. nili</i> ♂	0	0	0	0	0
Human malaria (incidence)	0.000	0.128	0.164	0.542	-
Human malaria (counts)	494	1341	1469	2893	24,978

TABLE 1 Summary statistics of the study populations. For *Anopheles*, the values are per trapping collection. For malaria, the values are for the whole year 2018. ♂ Males and ♀ females.

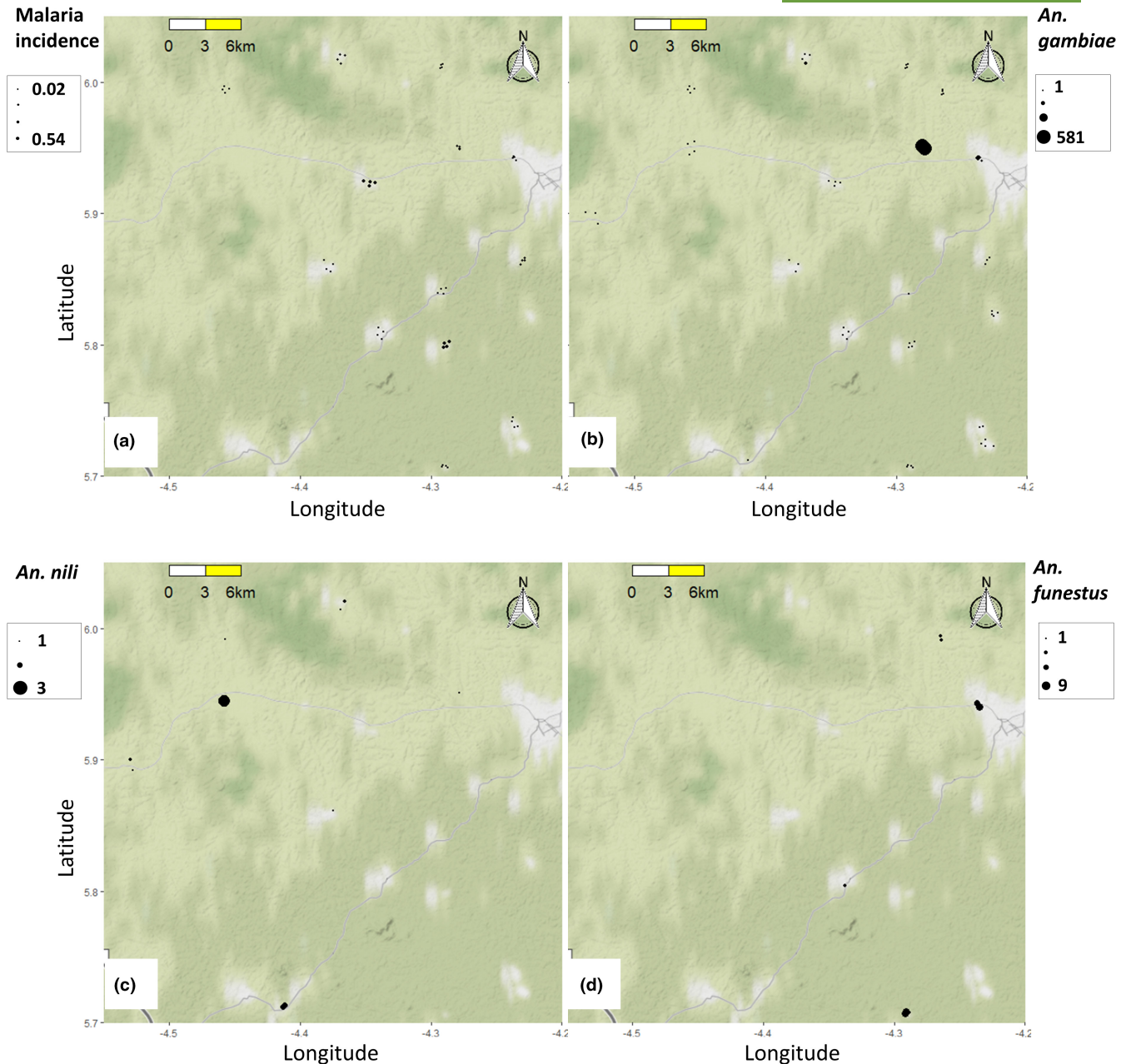


FIGURE 3 Total number of mosquitoes (female) collected in each house during the survey for *An. gambiae* (b), *An. nili* (c) and *An. funestus* (d). Top-left map (a) shows malaria incidence in the villages (not for all the villages the malaria information was available).

3.3 | The common spatial process for vectors and malaria

As described in the methods, the four models had common spatial and pure error effects. Their inference was obtained via maximum likelihood estimation (Figure 2). The common spatial component had a range (defined as the limit for the decay function to control the local variance) of 0.125 (Table 2) equivalent to approximately 14 km. The strong spatial autocorrelation (in other words the variance that is spatially dependent) can be deduced from the nugget to sill ratio (Cressie, 2015). Here, the proportion of the pure error (nugget effect) of the total variance (partial sill + nugget effect) is

6%; therefore, 94% of the variance (not explained by the predictors or fixed effects) depends on the location.

3.4 | Model evaluation and validation

The spatial variance explained a large part of the variation for *An. nili*, almost 48% of the sample variance, but not for malaria incidence, which is only 8% given the common 6% of nugget (Tables 2 and 3).

The left-out 15% of the data had the vector species and malaria incidence spatial dependences within the 95% confidence interval of

the ones of the entire data (see [Figure S2](#)). Therefore, the data used for cross validation are representative of the real data.

The model with most uncertainty was the one for *An. gambiae* (highest ME, MSE and RMSE, and largest discrepancy of coverage to an ideal 95% for both 15% left-out and leave-one-village-out cross validation data) while the one with lowest uncertainty was *An. nili* ([Table 3](#)).

In the comparison between the joint modelling and four independent models, the latter presents larger increases in the RMSE from 10% for *An. gambiae* to 66% for malaria incidence ([Table 4](#)), which means that independent models are characterised by larger uncertainties at the point estimates. However, when considering predictions at village level (leave-one-village-out cross validation equivalent to an area block cross validation), the improvement is larger for *An. gambiae* and *An. nili* than for malaria incidence, for which improvement was 16% compared to 66% obtained from a random but spatially representative cross validation ([Table 4](#)).

3.5 | Suitability maps and co-regionalisation

Anopheles gambiae suitability is widespread compared to the other two *Anopheles* species ([Figure 4b](#) vs. [Figure 4c,d](#)), with most areas coincident with suitability for malaria incidence ([Figure 4a](#)). As expected, residuals (see [Figure S3](#)) have larger values in areas with close proximity between high and low mosquito counts and malaria incidence values (or vice versa).

Maps of positive correlation between suitability of malaria and *Anopheles* cover most of the region ([Figure 5a](#)). Most of the areas show significant correlation between two vectors and malaria incidence suitabilities. There is a band crossing south-west-centre to north which is highly suitable to all three vectors and correlated to malaria incidence suitability ([Figure 5a](#)). Mosquito residuals are also correlated with malaria but less geographically extended than the fitted values ([Figure 5a](#) vs. [Figure 5b](#), and see [Figure S4](#)). The areas where large residuals from mosquito and malaria models correlate

Process	Model parameter	2.50%	Mean	97.50%
<i>An. gambiae</i>	Intercept	35.871	41.873	48.185
	Land cover=forest	Ref.	Ref.	Ref.
	Land cover=grassland	0.012	0.048	0.094
	MODIS_Ta	0.004	0.005	0.006
	Wind speed	-0.444	-0.226	-0.008
	Elevation	-0.024	-0.020	-0.017
<i>An. funestus</i>	Intercept	0.012	0.031	0.054
	ws_Tmin	0.064	0.069	0.074
	MU	0.009	0.011	0.013
<i>An. nili</i>	Intercept	0.052	0.155	0.356
	ws_Tmax	0.044	0.059	0.074
Malaria incidence	Intercept	-13.011	-9.305	-5.570
	Modis_Ta	0.011	0.015	0.023
	Modis_EVla	0.013	0.015	0.019
	AG	0.007	0.301	0.506
Joint parameters	Spatial range	0.121	0.125	0.128
	Nugget effect	0.177	0.348	0.405
	Partial sill	4.940	5.353	5.425

TABLE 2 Model parameters' inference results. Mean and 95% credible interval are shown for each model parameter. Legend: MODIS land surface temperature amplitude (Modis_Ta), weekly weather station wind speed (Wind speed), weekly weather station minimum temperature (ws_Tmin), female *Mansonia uniformis* (MU) counts, weekly weather station maximum temperature (ws_Tmax), MODIS enhanced vegetation index amplitude (Modis_EVla) and female *An. gambiae* (AG) counts.

TABLE 3 Model evaluation (ME and MSE) and validation (Coverage and RMSE) statistics. Explained variance from the fixed effects (predictors) component is shown in the last column.

Process	ME	MSE	COV (%) ^a	COV (%) ^b	RMSE ^a	RMSE ^b	Explained variance by the fixed effect (%)
<i>An. gambiae</i>	0.292	1.173	83.33	90.59	1.086	0.910	53.385
<i>An. funestus</i>	-0.034	0.134	93.33	97.35	0.278	0.100	70.936
<i>An. nili</i>	0.002	0.087	100	98.82	0.009	0.048	46.299
Malaria incidence	0.183	0.744	100	97.50	0.003	0.914	86.604

^aStatistics based on out-of-sample cross validation.

^bStatistics based on leave-one-village-out cross validation.

TABLE 4 Model validation (Coverage and RMSE) statistics for the independent models.

Process	COV (%) independent models	RMSE independent models	COV (%) independent models ^a	RMSE independent models ^a	Difference in RMSE compared to joint model
<i>An. gambiae</i>	83.33	1.196	90.00	1.111	+10% +22% ^a
<i>An. funestus</i>	93.33	0.277	97.36	0.096	-0.4% -4% ^a
<i>An. nili</i>	100	0.014	98.82	0.068	+55% +41% ^a
Malaria incidence	100	0.005	83.33	1.064	+66% +16% ^a

^aStatistics based on leave-one-village-out cross validation.

positively can likely be attributed to factors not considered in the analysis.

4 | DISCUSSION

The proposed modelling framework has three advantages: (i) production of malaria and mosquito suitability maps simultaneously including within sampled area and nearby areas where information is not currently available, and for which covariances between outputs are estimated; (ii) identification of the common spatial effects in environmental suitability for mosquitoes and malaria; and (iii) estimation of the geographic shared and correlated components (fitted and residuals) between mosquito species and malaria suitabilities (co-regionalisation), which allows spatial identification of important, but unquantified, sources of variation.

In this analysis, we have shown that by joint modelling vectors and malaria it is possible to delineate regions where one or more vector suitability correlated with malaria suitability implicating the risk of unsuccessful species-specific interventions (Deredec et al., 2016), and regions where their residuals correlated—indicating the presence of shared risk factors not included in the study but that if found, can contribute to the interventions aimed to break the malaria transmission pathway. The estimated correlations between outcomes from the joint model are unbiased compared to those obtained by simple correlation of outputs from individual modelling (Efthimiou et al., 2014; Ishak et al., 2008). In addition, the joint model was able to reduce the variance in the estimates compared to individual and independent models, stressing the importance of considering common components (the spatial correlation component ω in this study) within the joint model.

The spatially correlated suitabilities between vectors and malaria covered most of the region (Figure 5a) supporting the malaria endemicism in the area. This has important consequences for malaria control. First, the heterogeneous distribution of the suitabilities indicates that broadly targeted interventions may produce different results (more effective where the transmission is weak—e.g. areas with low suitability for both malaria and vectors, and relatively less for areas with strong transmission). This suggests that geographically

targeted interventions may be better suited for this region (Canelas et al., 2021). Second, intervening in areas where only one species suitability is associated with malaria suitability or where in general the suitability is low may be the priority for progressive elimination. Current results indicate that interventions progressing east to west and/or west to east, from the periphery to the centre as in a 'fried egg' design (Manrique-Saide et al., 2020), may provide better results than those along the axes south–north, or allocated randomly or uniformly. Third, and more importantly, the area is dominated by correlated suitabilities between malaria and more than one vector, which could lead to failure of any species-specific interventions (Deredec et al., 2016).

The mapping of co-regionalised residuals (regions where suitability residuals from a vector and suitability residuals from malaria overlap and correlate) is highly intense in several spots of the area. These areas are likely to be the results of model-correlated uncertainties or predictors not considered in this study and that act at both vector and malaria level but also to factors indirectly related to the distribution of the mosquitoes (human behaviour, human mobility, house construction, etc.; Guerra et al., 2019; Sedda et al., 2022). Investigating the areas with large vector-malaria-correlated residuals is necessary not only to target additional surveillance (in order to improve distribution maps) but also to identify hidden predictors of malaria and mosquito suitability that can improve knowledge in malaria transmission risk factors (Handique et al., 2016; Zhou et al., 2007) and inform the future direction for malaria prevention, control and elimination. To identify these factors, areas of high malaria suitability and highly correlated vector-malaria suitability residuals must be prioritised for investigation (Cavany et al., 2023; Cohen et al., 2017).

Our study allowed for model-specific environmental effects between mosquitoes, and between mosquitoes and malaria incidence, revealing shared and unshared risk factors between the vectors and malaria typical for Côte d'Ivoire (M'Bra et al., 2018; Zogo et al., 2019; Zoh et al., 2020). Results support other studies that describe the key role of temperature upon the suitability of *Anopheles species* (Afrane et al., 2012; Beck-Johnson et al., 2013). Contrary to previous studies, rainfall was not found important, a result that can be found elsewhere (Darkoh et al., 2017; Gilioli &

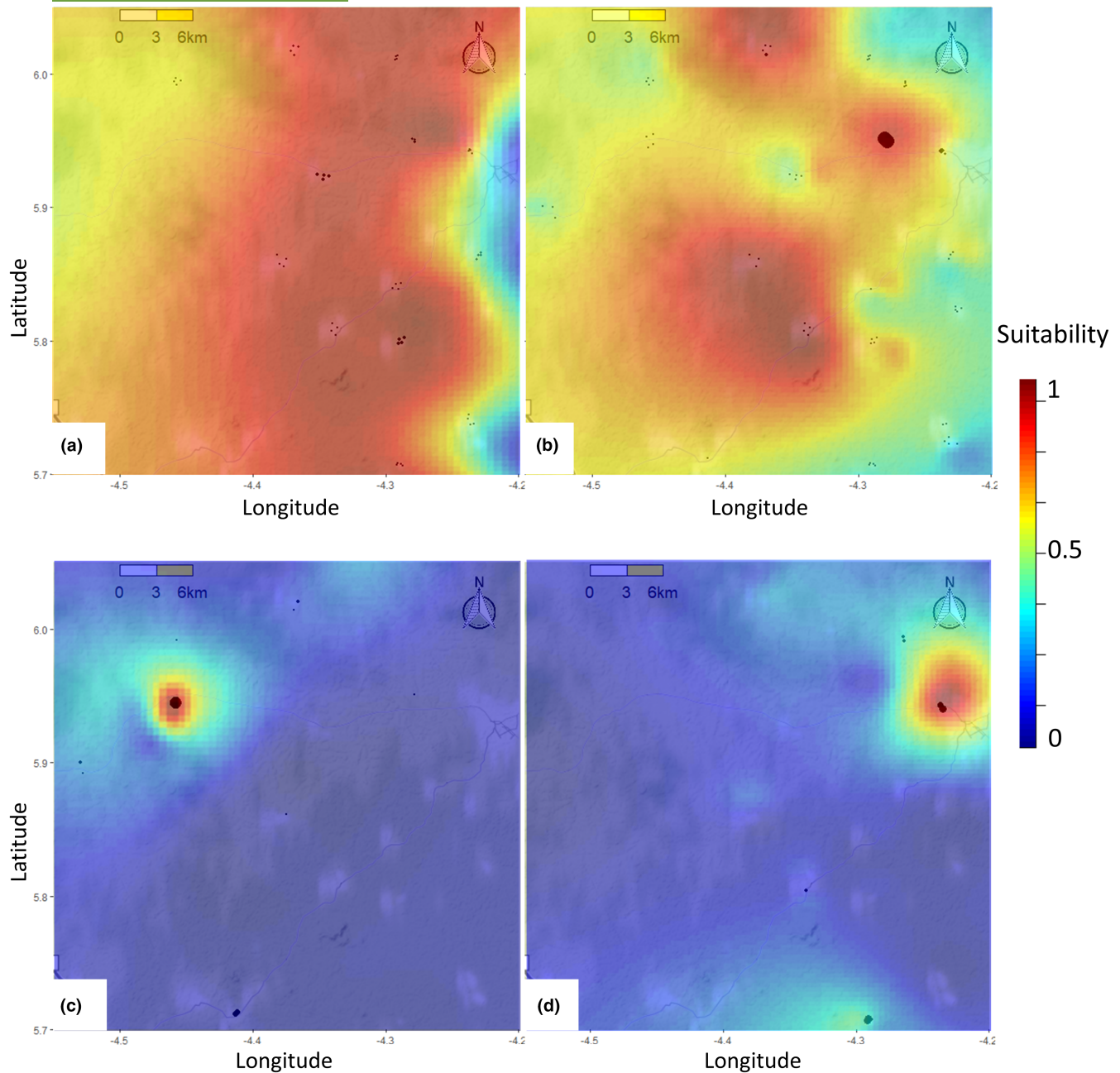


FIGURE 4 Suitability maps for malaria incidence (a), *An. gambiae* (b), *An. nili* (c) and *An. funestus* (d). Suitability maps overlaid over [Figure 3](#) showing total counts. Plot created with function `image.plot` from the 'fields' package of R-cran software. Maps standard errors are provided in [Figure S3](#).

Mariani, 2011). Although rainfall has a significant role in mosquito development via creation of breeding sites, it is possible that the spatial resolution for the rain variable was not sufficient to describe the spatial variation of mosquito abundance (Obsomer et al., 2013) due to sampling carried out over the wet season, and therefore lacking in variation.

As we found, *An. gambiae* has been determined to be the major risk factor for malaria incidence elsewhere (Zoh et al., 2020). The strong spatial association between *An. gambiae* and malaria and less spatial association between *An. funestus* and malaria have also been previously documented in Côte d'Ivoire (Nzeyimana et al., 2002).

There are several caveats to be noted when interpreting this study. When predicting at village level, while *An. gambiae*, *An. nili* and malaria incidence improved the RMSE, the two mosquito species had larger improvements in accuracy from the joint model compared to the malaria incidence, potentially indicating the lack of contribution of the small-scale effects at village level. In fact, these two species show shorter individual spatial scales than the malaria one (see [Figure S2](#)), that is still larger than the one estimated and accounted by the joint space modelling (Maurer & Taper, 2002). The same reason can be attributed to the slight loss of improvement for *An. funestus* during the leave-one-village-out cross validation. Despite

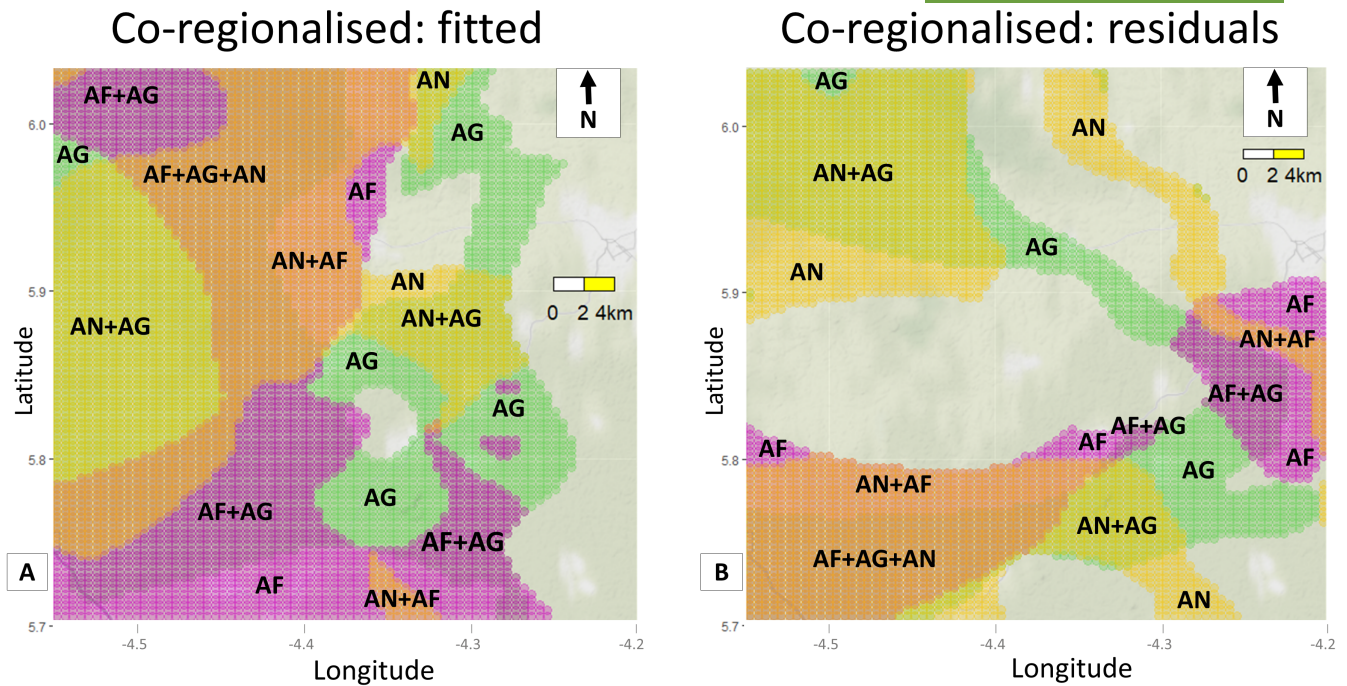


FIGURE 5 Co-regionalisation analysis for model estimations (a) and residuals (b). Different colours indicate areas where one or more *Anopheles* species (AG, *An. Gambiae*; AF, *An. Funestus*; and AN, *An. nili*) and malaria suitability are above 0.25, with correlation between the single species and malaria above 0.1. Map was created with 'ggmap' and 'ggsp' packages in R-cran software; basemap and data from OpenStreetMap under the Open Database licence (<https://www.openstreetmap.org/copyright>).

this trade-off, in general the joint modelling improved the accuracy of the estimation compared to individual modelling. Although other hierarchical models can provide a better estimate of the individual spatial autocorrelation parameters (König et al., 2021), this was not the scope of this work which was targeting the common spatial effects that enabled the improvement of the joint model performance. The short period of collection may have contributed to the high spatial heterogeneity and affected the robustness of the variable selection process. In addition, malaria incidence was not available for all the locations for which we had entomological data, and it was provided for the full year rather than for the exact period of mosquito surveillance. The absence of information for some locations is accounted for by the spatial modelling approach (estimation of missing data is performed by the model). The use of the annual malaria incidence data, due to the absence of weekly and monthly information, relies on the assumption that malaria incidence is representative of the relative malaria intensity in the area. Under this assumption, it is expected that the differences in malaria incidence between two villages should not change during the year given the relatively small spatial scale of the study.

Public health centres can be biased towards the local malaria burden due to the accessibility of the centres for their neighbouring populations (N'goran Kone et al., 2019), causing uncertainty on the true denominator used to calculate the incidence rates. There is no information about village-level biases in malaria reporting for Côte d'Ivoire that can be included in the model, therefore the statistical analyses were carried out in accordance with the methodology advised for the use of routine health information system data

(Ashton et al., 2017), including the use of confirmed malaria cases instead of suspected cases. It is also important to stress that this study focusses on estimating the common variance between the models, and biases affecting the variance can be reduced by considering covariates (environmental, climatic, etc.) at higher resolution than the outcomes (mosquito counts and malaria incidence) (Paciorek, 2010), as done in this study. The model choice and assumptions (including priors), especially with limited data, can influence model inference—that is level of smoothness and uncertainty. While the spatial extent is relatively small (60 by 60 km), the ecological and malaria conditions are typical for the south-centre Côte d'Ivoire, which is dominated by tropical and subtropical moist broadleaf forests biome (Schapira & Boutsika, 2012). The dominant malaria vectors are typical of the wider Afrotropical region (Schapira & Boutsika, 2012), meaning the potential to extend the predictions beyond south-central Côte d'Ivoire. However, spatial analyses have the disadvantage that their scales are influenced by local factors (human behaviour and movements, landscape fragmentation, public health interventions, to name a few) limiting their generalizability beyond areas with similar ecological and epidemiological conditions. A likely indicator of the presence of these local factors not included in this study is the range of 14 km, a spatial scale much larger than common mosquito flight distances (Sedda et al., 2022).

Finally, we used only a restricted set of environmental variables which may cause over-estimation of the random effects. Based on these limitations, follow-up studies with longer repeated measurements over time and with larger spatial scales are needed. Despite these limitations, this work serves as an example procedure to

identify areas and risk factors associated with the shared spatial effects and correlated residuals and that can inform the scale and intensity of the allocation of vector interventions (e.g. prioritising areas; Odhiambo et al., 2020; Poggiato et al., 2021). The need for these models is twofold: from a statistical point of view to improve prediction at local scales and identify unexplained variation for further investigation; and on the policy side, to support community-based malaria case management.

AUTHOR CONTRIBUTIONS

All authors conceived the ideas; Martin James Donnelly, David Weetman and Luigi Sedda designed methodology; Ruth Marie A. Kouame and Ako V. Constant Edi collected the data; Luigi Sedda and Russell John Cain analysed the data; Luigi Sedda and Ruth Marie A. Kouame led the writing of the manuscript. All authors contributed critically to the drafts and gave final approval for publication. Our study brings together authors from a number of different countries, including scientists, at different stage in their own career, based in the country where the study was carried out. All authors were engaged early on with the research and study design to ensure that the diverse sets of perspectives they represent were considered from the onset. Whenever relevant, literature published by scientists from the region was cited; efforts were made to consider relevant work published in the local language. Our research was discussed with local and other African stakeholders to seek feedback on the questions to be tackled and the approach to be considered.

ACKNOWLEDGEMENTS

We are grateful to the villages' chiefs, who made it possible to conduct the study in their communities. We thank all the field workers in each village who helped us in houses selection and mosquitoes' collection; and not least the residents who accepted to receive us in their houses.

FUNDING INFORMATION

This work was funded the Medical Research Council (MR/P02520X/1). This grant is a UK-funded award and is part of the EDCTP2 Programme supported by the European Union. Additional support was provided by the Wellcome Trust NIHR-Wellcome Partnership for Global Health Research Collaborative Award, CEASE (220870/Z/20/Z). M.J.D. and R.M.A.K. were supported by a Royal Society Wolfson Fellowship (RSWF\FT\180003). The funders had no role in study design and analysis, decision to publish or the preparation of the manuscript.

CONFLICT OF INTEREST STATEMENT

We declare no competing interests.

DATA AVAILABILITY STATEMENT

Entomological data are available from the Zenodo repository <https://doi.org/10.5281/zenodo.8300532> (Kouame & Edi, 2023). Malaria data are available through local health services by contacting the local head of health department. Model code is available from the

Zenodo repository <https://doi.org/10.5281/zenodo.10258689> (Sedda, 2023).

ORCID

Martin James Donnelly  <https://orcid.org/0000-0001-5218-1497>

Luigi Sedda  <https://orcid.org/0000-0002-9271-6596>

REFERENCES

- Adja, A. M., N'Goran, E., K., Koudou, B. G., Dia, I., Kengne, P., Fontenille, D., & Chandre, F. (2011). Contribution of *Anopheles funestus*, *An. gambiae* and *An. nili* (Diptera: Culicidae) to the perennial malaria transmission in the southern and western forest areas of Cote d'Ivoire. *Annals of Tropical Medicine and Parasitology*, 105, 13–24. <https://doi.org/10.1179/136485910X12851868780388>
- Afrane, Y. A., Githeko, A. K., Yan, G. (2012). The ecology of *Anopheles* mosquitoes under climate change: case studies from the effects of deforestation in East African highlands. *Annals of the New York Academy of Sciences*. 2012 Feb; 1249, 204–10. <https://doi.org/10.1111/j.1749-6632.2011.06432.x>.
- AlShammari, T., Elgabli, A., & Bennis, M. (2021). MetaBayes: A meta-learning framework from a Bayesian perspective. In *2021 55th Asilomar Conference on Signals, Systems, and Computers*. (pp. 351–355). Institute of Electrical and Electronics Engineers (IEEE). <https://doi.org/10.1109/IEEECONF53345.2021.9723290>
- Arab, A., Jackson, M. C., & Kongoli, C. (2014). Modelling the effects of weather and climate on malaria distributions in West Africa. *Malaria Journal*, 13, 126. <https://doi.org/10.1186/1475-2875-13-126>
- Ashton, R. A., Bennett, A., Yukich, J., Bhattarai, A., Keating, J., & Eisele, T. P. (2017). Methodological considerations for use of routine health information system data to evaluate malaria program impact in an era of declining malaria transmission. *American Journal of Tropical Medicine and Hygiene*, 97, 46–57. <https://doi.org/10.4269/ajtmh.16-0734>
- Attoumane, A., Silai, R., Bacar, A., Cardinale, E., Pennober, G., & Herbreteau, V. (2020). Changing patterns of malaria in Grande Comore after a drastic decline: Importance of fine-scale spatial analysis to inform future control actions. *Remote Sensing*, 12, 4082. <https://doi.org/10.3390/rs12244082>
- Beck-Johnson, L. M., Nelson, W. A., Paaijmans, K. P., Read, A. F., Thomas, M. B., Bjørnstad, O. N. (2013). The Effect of Temperature on *Anopheles* Mosquito Population Dynamics and the Potential for Malaria Transmission. *PLOS ONE* 8(11), e79276. <https://doi.org/10.1371/journal.pone.0079276>
- Becker, N., Petric, D., Zgomba, M., Boase, C., Madon, M., Dahl, C., & Kaiser, A. (2010). *Mosquitoes and their control*. Springer Science & Business Media.
- Canelas, T., Thomsen, E., McDermott, D., Sternberg, E., Thomas, M. B., & Worrall, E. (2021). Spatial targeting of screening + eave tubes (SET), a house-based malaria control intervention, in Côte d'Ivoire: A geostatistical modelling study. *PLOS Global Public Health*, 1, e0000030. <https://doi.org/10.1371/journal.pgph.0000030>
- Cavany, S., Huber, J. H., Wieler, A., Tran, Q. M., Alkuzweny, M., Elliott, M., España, G., Moore, S. M., & Perkins, T. A. (2023). Does ignoring transmission dynamics lead to underestimation of the impact of interventions against mosquito-borne disease? *BMJ Global Health*, 8, e012169. <https://doi.org/10.1136/bmjgh-2023-012169>
- Cohen, J. M., Le Menach, A., Pothin, E., Eisele, T. P., Gething, P. W., Eckhoff, P. A., Moonen, B., Schapira, A., & Smith, D. L. (2017). Mapping multiple components of malaria risk for improved targeting of elimination interventions. *Malaria Journal*, 16, 459. <https://doi.org/10.1186/s12936-017-2106-3>
- Cressie, N. (2015). *Statistics for spatial data*. John Wiley & Sons.

- Darkoh, E. L., Larbi, J. A., & Lawer, E. A. (2017). A weather-based prediction model of malaria prevalence in Amenfi West District, Ghana. *Malaria Research and Treatment*, 2017, 7820454.
- Deredec, A., O'Loughlin, S. M., Hui, T.-Y. J., & Burt, A. (2016). Partitioning the contributions of alternative malaria vector species. *Malaria Journal*, 15(60), 127. <https://doi.org/10.1186/s12936-016-1107-y>
- Dormann, C. F., Elith, J., Bacher, S., Buchmann, C., Carl, G., Carré, G., Marquéz, J. R. G., Gruber, B., Lafourcade, B., Leitão, P. J., Münkemüller, T., McClean, C., Osborne, P. E., Reineking, B., Schröder, B., Skidmore, A. K., Zurell, D., & Lautenbach, S. (2013). Collinearity: A review of methods to deal with it and a simulation study evaluating their performance. *Ecography*, 36, 27–46. <https://doi.org/10.1111/j.1600-0587.2012.07348.x>
- Dossou-yovo, J., Doannio, J. M., Rivièrè, F., & Chauvancy, G. (1995). Malaria in Côte d'Ivoire wet savannah region: The entomological input. *Tropical Medicine and Parasitology*, 46, 263–269.
- Efthimiou, O., Mavridis, D., Cipriani, A., Leucht, S., Bagos, P., & Salanti, G. (2014). An approach for modelling multiple correlated outcomes in a network of interventions using odds ratios. *Statistics in Medicine*, 33, 2275–2287. <https://doi.org/10.1002/sim.6117>
- Finley, A. O., Banerjee, S., & Cook, B. D. (2014). Bayesian hierarchical models for spatially misaligned data in R. *Methods in Ecology and Evolution*, 5, 514–523. <https://doi.org/10.1111/2041-210x.12189>
- Finley, A. O., Bsneree, S., & Gelfand, A. E. (2015). spBayes for large univariate and multivariate point-referenced spatio-temporal data models. *Journal of Statistical Software*, 63, 1–28. <https://doi.org/10.18637/jss.v063.i13>
- Gelman, A., Hwang, J., & Vehtari, A. (2014). Understanding predictive information criteria for Bayesian models. *Statistics and Computing*, 24, 997–1016. <https://doi.org/10.1007/s11222-013-9416-2>
- Gilioli, G., & Mariani, L. (2011). Sensitivity of Anopheles gambiae population dynamics to meteo-hydrological variability: A mechanistic approach. *Malaria Journal*, 10, 294. <https://doi.org/10.1186/1475-2875-10-294>
- Gillies, M. T., & Coetzee, M. (1987). A supplement to the Anophelinae of Africa South of the Sahara. *Publications of the South African Institute for Medical Research*, 55, 1–143.
- Guerra, C. A., Kang, S. Y., Citron, D. T., Hergott, D. E. B., Perry, M., Smith, J., Phiri, W. P., Osá Nfumu, J. O., Mba Eyono, J. N., Battle, K. E., Gibson, H. S., García, G. A., & Smith, D. L. (2019). Human mobility patterns and malaria importation on Bioko Island. *Nature Communications*, 10, 2332. <https://doi.org/10.1038/s41467-019-10339-1>
- Handique, B. K., Khan, S. A., Dutta, P., Nath, M. J., Qadir, A., & Raju, P. L. N. (2016). Spatial correlations of malaria incidence hotspots with environmental factors in Assam, north East India. *Xxiii Ipsrs Congress, Commission VIII*, 3, 51–56. <https://doi.org/10.5194/ipsrs-annals-III-8-51-2016>
- Ishak, K. J., Platt, R. W., Joseph, L., & Hanley, J. A. (2008). Impact of approximating or ignoring within-study covariances in multivariate meta-analyses. *Statistics in Medicine*, 27, 670–686. <https://doi.org/10.1002/sim.2913>
- König, C., Wüest, R. O., Graham, C. H., Karger, D. N., Sattler, T., Zimmermann, N. E., & Zurell, D. (2021). Scale dependency of joint species distribution models challenges interpretation of biotic interactions. *Journal of Biogeography*, 48, 1541–1551. <https://doi.org/10.1111/jbi.14106>
- Kouame, R. M. A., & Edi, A. V. C. (2023). GAARDIAN mosquito collection Côte d'Ivoire. *Zenodo Repository*, 155 <https://doi.org/10.5281/zenodo.8300532>
- Lindsay, S. W., & Bayoh, M. N. (2004). Mapping members of the Anopheles gambiae complex using climate data. *Physiological Entomology*, 29, 204–209. <https://doi.org/10.1111/j.0307-6962.2004.00405.x>
- Liu, X., Chen, F., Lu, Y.-C., & Lu, C.-T. (2017). Spatial prediction for multivariate non-gaussian data. *ACM Transactions on Knowledge Discovery from Data (TKDD)*, 11, 1–27.
- Manrique-Saide, P., Dean, N. E., Halloran, M. E., Longini, I. M., Collins, M. H., Waller, L. A., Gomez-Dantes, H., Lenhart, A., Hladish, T. J., Che-Mendoza, A., Kirstein, O. D., Romer, Y., Correa-Morales, F., Palacio-Vargas, J., Mendez-Vales, R., Pérez, P. G., Pavia-Ruz, N., Ayora-Talavera, G., & Vazquez-Prokopec, G. M. (2020). The TIRS trial: Protocol for a cluster randomized controlled trial assessing the efficacy of preventive targeted indoor residual spraying to reduce Aedes-borne viral illnesses in Merida, Mexico. *Trials*, 21, 839. <https://doi.org/10.1186/s13063-020-04780-7>
- Maurer, B. A., & Taper, M. L. (2002). Connecting geographical distributions with population processes. *Ecology Letters*, 5, 223–231. <https://doi.org/10.1046/j.1461-0248.2002.00308.x>
- M'Bra, R. K., Kone, B., Soro, D. P., N'krumah, R. T. A. S., Soro, N., Ndione, J. A., Sy, I., Ceccato, P., Ebi, K. L., Utzinger, J., Schindler, C., & Cisse, G. (2018). Impact of climate variability on the transmission risk of malaria in northern Cote d'Ivoire. *PLoS One*, 13, e0182304. <https://doi.org/10.1371/journal.pone.0182304>
- Meyer, H., Reudenbach, C., Hengl, T., Katurji, M., & Nauss, T. (2018). Improving performance of spatio-temporal machine learning models using forward feature selection and target-oriented validation. *Environmental Modelling & Software*, 101, 1–9. <https://doi.org/10.1016/j.envsoft.2017.12.001>
- Meyer, H., Reudenbach, C., Wöllauer, S., & Nauss, T. (2019). Importance of spatial predictor variable selection in machine learning applications—Moving from data reproduction to spatial prediction. *Ecological Modelling*, 411, 108815. <https://doi.org/10.1016/j.ecolm.odel.2019.108815>
- N'goran Kone, L. F., N'Dia, F. A., & N'Goran, A. G. (2019). Determinants of therapeutic routes for malaria patients in Ivory Coast. *Utafiti*, 14, 75–91. <https://doi.org/10.1163/26836408-14010004>
- Noor, A. M., & Alonso, P. L. (2022). The message on malaria is clear: Progress has stalled. *Lancet*, 399, 1777. [https://doi.org/10.1016/S0140-6736\(22\)00732-2](https://doi.org/10.1016/S0140-6736(22)00732-2)
- Nzeyimana, I., Henry, M. C., Dossou-Yovo, J., Doannio, J. M. C., Diawara, L., & Carnevale, P. (2002). Malaria epidemiology in the south-western forest area of Cote d'Ivoire (region of tai). *Bulletin de la Societe de Pathologie Exotique*, 95, 89–94.
- Obsomer, V., Titeux, N., Vancustem, C., Duveiller, G., Pekel, J., Connor, S., Ceccato, P., & Coosemans, M. (2013). From Anopheles to spatial surveillance: A roadmap through a multidisciplinary challenge. *Anopheles Mosquitoes—New Insights into Malaria Vectors*, 140.
- Odhiambo, J. N., Kalinda, C., Macharia, P. M., Snow, R. W., & Sartorius, B. (2020). Spatial and spatio-temporal methods for mapping malaria risk: A systematic review. *BMJ Global Health*, 5, e002919. <https://doi.org/10.1136/bmjgh-2020-002919>
- Paciorek, C. J. (2010). The importance of scale for spatial-confounding bias and precision of spatial regression estimators. *Statistical Science*, 25, 107–125. <https://doi.org/10.1214/10-sts326>
- Ploton, P., Mortier, F., Réjou-Méchain, M., Barbier, N., Picard, N., Rossi, V., Dormann, C., Cornu, G., Viennois, G., Bayol, N., Lyapustin, A., Gourlet-Fleury, S., & Pélissier, R. (2020). Spatial validation reveals poor predictive performance of large-scale ecological mapping models. *Nature Communications*, 11, 4540. <https://doi.org/10.1038/s41467-020-18321-y>
- Plummer, M., Best, N., Cowles, K., & Vines, K. (2006). CODA: Convergence diagnosis and output analysis for MCMC. *R News*, 6, 7–11.
- Poggiato, G., Münkemüller, T., Bystrova, D., Arbel, J., Clark, J. S., & Thuiller, W. (2021). On the interpretations of joint modeling in community ecology. *Trends in Ecology & Evolution*, 36, 391–401. <https://doi.org/10.1016/j.tree.2021.01.002>
- Roberts, D. R., Bahn, V., Ciuti, S., Boyce, M. S., Elith, J., Guillera-Aroita, G., Hauenstein, S., Lahoz-Monfort, J. J., Schröder, B., Thuiller, W., Warton, D. I., Wintle, B. A., Hartig, F., & Dormann, C. F. (2017). Cross-validation strategies for data with temporal, spatial, hierarchical, or phylogenetic structure. *Ecography*, 40, 913–929. <https://doi.org/10.1111/ecog.02881>

- Rosenthal, J. S. (2007). AMCMC: An R interface for adaptive MCMC. *Computational Statistics & Data Analysis*, 51, 5467–5470. <https://doi.org/10.1016/j.csda.2007.02.021>
- Russell, T. L., Lwetoijera, D. W., Knols, B. G. J., Takken, W., Killeen, G. F., & Kelly-Hope, L. A. (2013). Geographic coincidence of increased malaria transmission hazard and vulnerability occurring at the periphery of two Tanzanian villages. *Malaria Journal*, 12, 24. <https://doi.org/10.1186/1475-2875-12-24>
- Sahu, S. (2022). *Bayesian modeling of spatio-temporal data with R*. CRC Press.
- Schapiro, A., & Boutsika, K. (2012). Malaria ecotypes and stratification. *Advances in Parasitology*, 78, 97–167. <https://doi.org/10.1016/B978-0-12-394303-3.00001-3>
- Sedda, L. (2023). Framework for joint Gaussian spatial processes (1.0.0). *Zenodo Repository*, 156 <https://doi.org/10.5281/zenodo.10258689>
- Sedda, L., Lucas, E. R., Djogbenou, L. S., Edi, A. V. C., Egyir-Yawson, A., Kabula, B. I., Midega, J., Ochomo, E., Weetman, D., & Donnelly, M. J. (2019). Improved spatial ecological sampling using open data and standardization: An example from malaria mosquito surveillance. *Journal of the Royal Society Interface*, 16, 20180941. <https://doi.org/10.1098/rsif.2018.0941>
- Sedda, L., McCann, R. S., Kabaghe, A. N., Gowelo, S., Mburu, M. M., Tizifa, T. A., Chipeta, M. G., van den Berg, H., Takken, W., van Vugt, M., Phiri, K. S., Cain, R., Tangena, J.-A. A., & Jones, C. M. (2022). Hotspots and super-spreaders: Modelling fine-scale malaria parasite transmission using mosquito flight behaviour. *PLoS Pathogens*, 18, e1010622. <https://doi.org/10.1371/journal.ppat.1010622>
- Tchicaya, A. F., Wognin, S. B., Aka, I. N. A., Kouassi, Y. M., Guiza, J., & Bonny, J. S. (2014). Impacts professionnels et économiques du paludisme à *Plasmodium falciparum* sur une entreprise du secteur privé en Côte d'Ivoire. *Archives des Maladies Professionnelles et de l'Environnement*, 75, 406–411. <https://doi.org/10.1016/j.admp.2014.02.005>
- Vehtari, A., Gelman, A., & Gabry, J. (2017). Practical Bayesian model evaluation using leave-one-out cross-validation and WAIC. *Statistics and Computing*, 27, 1413–1432. <https://doi.org/10.1007/s1122-016-9696-4>
- World Health Organization. (2019). *World malaria report 2019*. World Health Organization.
- World Health Organization. (2020). *World malaria report 2020: 20 years of global progress and challenges*. In *World malaria report 2020: 20 years of global progress and challenges* (p. 299). World Health Organization.
- World Health Organization. (2022). *World malaria report 2022*. World Health Organization.
- Zhou, G., Munga, S., Minakawa, N., Githeko, A. K., & Yan, G. (2007). Spatial relationship between adult malaria vector abundance and environmental factors in western Kenya highlands. *American Journal of Tropical Medicine and Hygiene*, 77, 29–35. <https://doi.org/10.4269/ajtmh.2007.77.29>
- Zogo, B., Soma, D. D., Tchiekoi, B. N., Somé, A., Ahoua Alou, L. P., Koffi, A. A., Fournet, F., Dahounto, A., Coulibaly, B., Kandé, S., Dabiré, R. K., Baba-Moussa, L., Moiroux, N., & Pennetier, C. (2019). Anopheles bionomics, insecticide resistance mechanisms, and malaria transmission in the Korhogo area, northern Côte d'Ivoire: A pre-intervention study. *Parasite*, 26, 40. <https://doi.org/10.1051/parasite/2019040>
- Zoh, D. D., Yapi, A., Adja, M. A., Guindo-Coulibaly, N., Kpan, D. M. S., Sagna, A. B., Adou, A. K., Cornelie, S., Brengues, C., Poinsignon, A., & Chandre, F. (2020). Role of *Anopheles gambiae* s.s. and *Anopheles coluzzii* (Diptera: Culicidae) in human malaria transmission in rural areas of Bouaké, in Côte d'Ivoire. *Journal of Medical Entomology*, 57, 1254–1261. <https://doi.org/10.1093/jme/tjaa001>

SUPPORTING INFORMATION

Additional supporting information can be found online in the Supporting Information section at the end of this article.

Figure S1. Temporal variation of total counts for female *An. gambiae* (A), *An. funestus* (B), and *An. nili* (C).

Figure S2. Theoretical variograms for the entire dataset (black lines) and 15% left-out data for cross validation (green lines).

Figure S3. Bayesian multivariate joint Gaussian spatial linear model residuals for each model.

Figure S4. Individual mosquito species – malaria co-regionalisation analysis for fitted values and residuals: correlation values.

Table S1. Explanatory variables data sources and properties.

Table S2. Summary statistics of the study population by village.

How to cite this article: Kouame, R. M. A., Edi, A. V. C., Cain, R. J., Weetman, D., Donnelly, M. J., & Sedda, L. (2023). Joint spatial modelling of malaria incidence and vector's abundance shows heterogeneity in malaria-vector geographical relationships. *Journal of Applied Ecology*, 00, 1–14. <https://doi.org/10.1111/1365-2664.14565>